




Received June 8, 2020; revised August 16, 2020; accepted August 25, 2020; date of publication September 10, 2020;  
date of current version October 6, 2020.

Digital Object Identifier 10.1109/TQE.2020.3023338

# Experimental Characterization, Modeling, and Analysis of Crosstalk in a Quantum Computer

ABDULLAH ASH- SAKI<sup>1</sup>  (Student Member, IEEE),  
MAHABUBUL ALAM<sup>1</sup>  (Student Member, IEEE),  
AND SWAROOP GHOSH<sup>1</sup>  (Senior Member, IEEE)

<sup>1</sup>Pennsylvania State University, University Park, PA 16802 USA

Corresponding author: Abdullah Ash- Saki. (axs1251@psu.edu)

This work was supported in part by the National Science Foundation under Grants CNS- 1722557, CCF-1718474, DGE-1723687, and DGE-1821766 and in part by seed grants from the Penn State Institute for Computational and Data Sciences and Huck Institute of the Life Sciences.

**ABSTRACT** In this article, we present the experimental characterization of crosstalk in quantum information processor using idle tomography and simultaneous randomized benchmarking. We quantify both “quantum” and “classical” crosstalk in the device and analyze quantum circuits considering crosstalk. We show that simulation considering only gate-error deviates from experimental results up to 27%, whereas simulation considering both gate error and crosstalk match the experiments more accurately with an average mismatch as low as 4.52%. This article enables simulation of quantum circuits with experimental crosstalk error rates.

**INDEX TERMS** Crosstalk, idle tomography, simultaneous randomized benchmarking, zz-interaction.

## I. INTRODUCTION

The Noisy Intermediate-Scale Quantum (NISQ) [1] computers are prone to gate error, readout error, decoherence, and crosstalk. Crosstalk is defined as the violation of “locality” and “independence” of (gate) operations [2]. Ideally, a gate should only affect the outcome of the qubit being operated. However, due to crosstalk, an operation on target qubit(s) may impact the non-target qubit(s). Several protocols have been presented in [2]–[11] to detect and benchmark crosstalk in Quantum Computers (QC). However, use-case of crosstalk in noisy quantum circuit simulation is not well explored with experimental error rates similar to gate errors. In this article, we demonstrate that consideration for crosstalk can lead to more accurate simulations of noisy quantum circuits. This can enable investigation of better noise resilience and circuit optimization techniques which take crosstalk into account (e.g., [12]) instead of prioritizing only gate errors. Besides, this article shows benefits of protocols like Simultaneous Randomized Benchmarking (SRB) [4] and Idle Tomography (IDT) [3], which quantifies crosstalk in terms of error rates similar to gate error rates, in simulating noisy quantum circuits.

**Contributions:** We, (i) employ two different experimental crosstalk characterization protocols, namely SRB and IDT, to extract crosstalk error rates in a QC (ibmq\_essex);

(ii) develop crosstalk model with extracted error rates; and (iii) simulate various quantum circuits/benchmarks with crosstalk error to demonstrate advantage of including crosstalk in noisy quantum circuit simulations.

## II. CROSSTALK IN NISQ DEVICES

In this section, we discuss physical reasons behind the presence of crosstalk in NISQ devices.

### A. QUANTUM CROSSTALK

Ideally, qubits are two-level systems. However, Transmon qubits have low anharmonicity which introduces higher-level states. The presence of higher-level states outside the computational  $|0\rangle$  and  $|1\rangle$  creates an always-on-ZZ interaction between two coupled qubits even-if they are not driven. In [15], the authors analytically show that the effective system Hamiltonian in the presence of higher levels is given by

$$H_{eff} = \omega_A \frac{ZI}{2} + \omega_B \frac{IZ}{2} + \xi \frac{ZZ}{2} \quad (1)$$

where the coefficient of the ZZ term  $\xi$  is given by

$$\xi = -\frac{J^2(\delta_A + \delta_B)}{(\Delta + \delta_A)(\delta_B - \Delta)}. \quad (2)$$

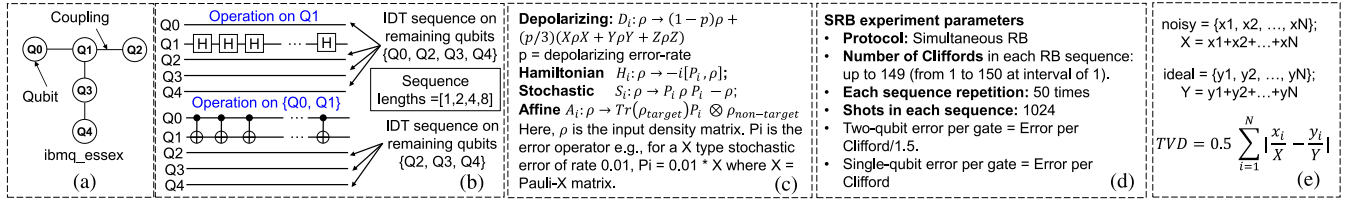


**FIG. 1.** (a) Coupling graph of 5-qubit `ibmq_essex`, (b) circuit construction for IDT experiments. IDT sequence list is generated using `pyGSTi` [13], [14], (c) equations for simulating various types of noise, (d) parameters used in the SRB experiments in this article, and (e) equation of total variation distance (TVD).

Here,  $J$  is exchange coupling strength between two qubits,  $\delta_{A/B}$  are the anharmonicities of qubits A and B, respectively, and  $\Delta$  is the frequency detuning (difference) of two coupled qubits. Fixed-frequency Transmons coupled to nearest neighbor have a static and nonzero value of  $J$ . Moreover, the strength of the cross-resonance drive (used to realize CNOT gate) is proportional to  $J$  [15], [16]. Thus, the nonzero  $J$  results in an always-on-ZZ interaction whether static or driven during cross-resonance gate. This always-on-ZZ-interaction gives rise to quantum crosstalk.

Due to the ZZ-interaction, the rotation rate of one qubit depends on the state of the other qubit, i.e., the rotation rate depends on another qubit being  $|0\rangle$  or  $|1\rangle$ . For device level or physical simulation, the strength of the ZZ-interaction ( $\xi$ ) can be measured using Ramsey experiment. However, for noisy quantum circuit simulation, the effect of ZZ-interaction in terms of “error rate” can be more appropriate.

### B. CLASSICAL CROSSTALK

Classical crosstalk may stem from incorrect control of the qubits. In [17], the authors presented multiple sources of classical crosstalk that can be present in Transmon-based quantum computers such as traditional electromagnetic (EM) crosstalk between microwave lines, stray on-chip EM fields, etc. On a high-level, the signal intended to control one qubit can disturb another independent qubit. For example, in [9] the authors demonstrate one such case where control fields (magnetic flux in this article) used to operate qubits have effect on un-addressed qubits. Physically, this can be modeled as changes in drive amplitude and phase as shown in [10]. The authors show the Hamiltonian for Transmon  $k$  with classical (also termed as “local” in [10]) crosstalk is given by

$$H_k = \omega_k \hat{n} + \frac{\alpha_k}{2} (\hat{n} - 1) \hat{n} + \sum_j \beta_{jk} \Omega_j(t) \cos(\omega_j t + \phi_j + \theta_{jk}) (\hat{a} + \hat{a}^\dagger) \quad (3)$$

The last term of (3) specifies the impact of excitation/drive applied on other qubits ( $j, j \neq k$ ) on the qubit  $k$ .  $\Omega_j(t)$  is the time dependent drive amplitude applied on qubit  $j$ , and  $\beta_{jk}$  is the scaling factor for classical crosstalk that determines how much drive on  $j$ th qubit perturbs the  $k$ th qubit. Similarly,  $\theta_{jk}$  is the phase lag added to the  $k$ th qubit due to crosstalk from drive on  $j$ th qubit.

## III. CROSSTALK ERROR RATE EXTRACTION

### A. IDLE TOMOGRAPHY

We run IDT circuits on a 5-qubit IBM QC (`ibmq_essex`). Using `pyGSTi` [13], [14], we create IDT circuits. IDT circuits prepare qubits in various initial states (Pauli eigenstate, e.g.  $|+\rangle$  state) and measure them in different Pauli bases (e.g., in X-basis). In between the state preparation and measurement, variable number of IDLE gates are added in qubits [3]. We create two types of circuits, namely “no-drive” and with “drive”. In no-drive case, IDT circuits created using `pyGSTi` run on all 5-qubits. The *drive* circuits are of two-types.

**i) Single-qubit drive:** A single-qubit gate (Hadamard gate in our experiments) is repeatedly applied on one qubit while IDT circuits are run on the remaining four qubits [Fig. 1(b)]. For example, IDT circuits run on Q0, Q2, Q3, and Q4 while Q1 is repeatedly driven by the Hadamard gate. We repeat this routine for all five qubits in the QC.

**ii) Two-qubit drive:** Similar to the single-qubit case, the CNOT gate is repeatedly applied on a pair of qubit while IDT circuits are run on the remaining three qubits [Fig. 1(b)]. For example, IDT circuits run on Q2, Q3, and Q4 while CNOT gates are applied on Q0 and Q1 pair. There are four coupled qubit pairs. We repeat this routine for all four of them. After both “no-drive” and “drive” circuits are created, they are executed on `ibmq_essex` with 8192 shots each and the “count” values are recorded. Note that, at the time of writing this article, public IBM devices allowed maximum 75 circuits (experiments) at once. Therefore, the complete list of IDT circuits is split into batches of 75 circuits each and scheduled on the `ibmq_essex`. Next, the count values from `ibmq_essex` are converted to `pyGSTi` compatible “dataset” and processed using `pyGSTi` to extract crosstalk error rates. Idle Tomography gives 3 types of crosstalk error rates, namely, Hamiltonian, Stochastic, and Affine [3]. Hamiltonian errors are the rotation (over/under) errors (in radian) along specific axis (e.g., X-axis). Stochastic errors specify the probability of Pauli X, Y, Z errors for single-qubit (or, XX, XY, XZ, YX, YY, YZ, ZX, ZY, ZZ errors for 2-qubit case). Affine errors work as a modifier for Stochastic errors. Finally, the extracted error rates are fed to a crosstalk model to simulate circuits [Fig. 1(c)].

The Python codes with exact details of the IDT circuit construction, execution on IBM machine, conversion to `pyGSTi` dataset, and postprocessing of the experimental data to extract error rates are included in the GitHub repository [18].

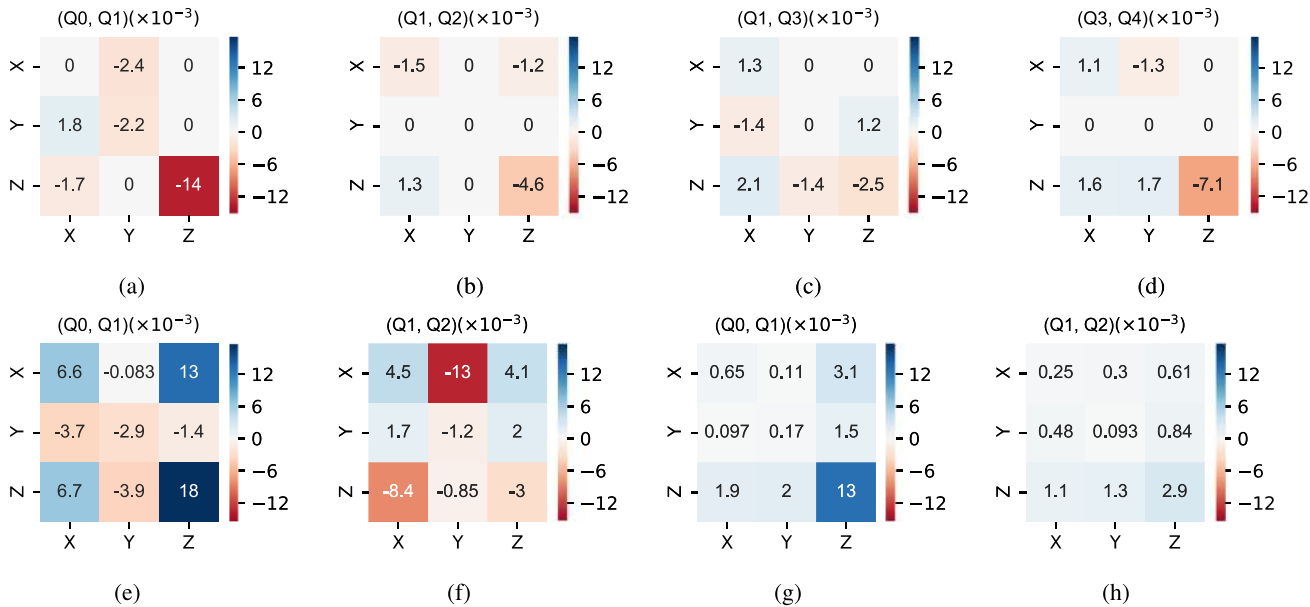


**FIG. 2.**  $H$  = Hamiltonian error and  $S$  = Stochastic error w/ drive values are extracted from experiments with repeated CNOT drive on Q3 and Q4. (For example, the value of  $13 \times 10^{-3}$  in Fig. 2(e) represents the error rate for X type error on Q0 and Z type error on Q1.). (a)  $H$  w/o drive. (b)  $H$  w/o drive. (c)  $H$  w/o drive. (d)  $H$  w/o drive. (e)  $H$  w/ drive on (Q3, Q4). (f)  $H$  w/ drive on (Q3, Q4). (g)  $S$  w/ drive on (Q3, Q4). (h)  $S$  w/ drive on (Q3, Q4).

**B. SIMULTANEOUS RANDOMIZED BENCHMARKING**

Next, we extract gate error rates with crosstalk using Simultaneous Randomized Benchmarking (SRB) [4]. SRB consists of applying RB sequences [19] to characterize multiple gate errors simultaneously. For example, CNOT(0, 1) and CNOT(3, 4) can be characterized together by running 2-qubit RB sequences on Qubit-0, 1 and Qubit-3, 4 simultaneously. Due to the simultaneous operation, any crosstalk between them will be reflected in the error rates. The parameters used in the SRB experiments in this article are listed in Fig. 1(d) and Python codes with exact details are in the GitHub repository [18]. We collect gate error for two simultaneous CNOT operations as well as isolated CNOT operations.

**IV. RESULTS AND DISCUSSION**

**A. CROSSTALK RATES FROM IDLE TOMOGRAPHY**

Fig. 2 shows weight-2 (acts on 2-qubit) Hamiltonian and Stochastic errors for both drive and no-drive cases. In no-drive case, we observe a higher ZZ-type Hamiltonian error compared to other types [Fig. 2(a)–(d)]. This indicates *quantum crosstalk* (Section II-A) which is due to always-on-ZZ-interaction in Transmon qubits [15]. Thus, IDT can pick up quantum crosstalk from residual ZZ-interactions. To further validate, we run Ramsey experiments on four possible qubit pairs. The results (Table I) show that pair (Q0, Q1) has the highest ZZ-interaction which supports the result from IDT. According to (2), the ZZ-interaction depends on exchange coupling strength  $J$ , frequency detuning  $\Delta$ , and anharmonicity  $\delta_{A/B}$ . Typically,  $J \ll |\Delta| < |\delta|$  [15], [20]. Detuning between Q0 and Q1 is higher (195.31 MHz from device specifications in [21]) than Q1 and Q2 (30.68 MHz [21]). Thus, the higher ZZ-interaction in (Q0, Q1) than (Q1, Q2) indicates the

**TABLE I** ZZ Interaction strength from Ramsey experiment

Qubit pair	ZZ interaction (kHz)
Q0, Q1	90.38
Q1, Q2	41.99
Q1, Q3	29.49
Q3, Q4	39.31

anharmonicities are playing a major role here in the quantum crosstalk in this case.

Note that, no-drive experiments show negligible Stochastic error and hence, are not plotted for brevity.

Next, we present IDT results with CNOT drive on (Q3, Q4) [Fig. 2(e)–(h)]. The difference between no-drive and drive results are indicative of *classical crosstalk* that impacts nontarget qubits (Q0, Q1, and Q2 in this case) due to operation on target qubits (Q3 and Q4). Operation on (Q3, Q4) introduces both Hamiltonian and Stochastic errors on the remaining qubits Q0, Q1, and Q2. We skip the complete set of error rates for brevity.

**B. CROSSTALK RATES FROM SIMULTANEOUS RANDOMIZED BENCHMARKING**

The results for two simultaneous CNOT operations are plotted in Fig. 3. Each bar represents the gate error rate for a CNOT gate either with or without an accompanying CNOT. The results show that in the presence of another CNOT gate, the gate error rates increase. For example, the error rate of CNOT(1,2) increases by 28.84% in the presence of simultaneous CNOT(3,4). This can be explained with (3). The increased error is due to spurious control field from the

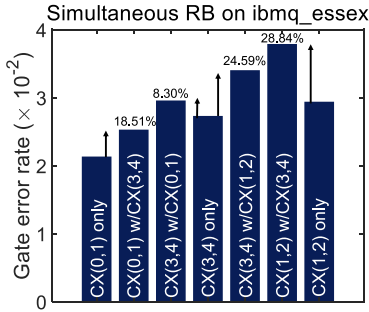


FIG. 3. CNOT gate error rates from SRB on ibmq\_essex.

neighboring pair [last term in (3)]. Crosstalk from neighboring qubits modifies the cross-resonance hamiltonian (CNOT gate hamiltonian). Hamiltonian tomography [20] can be utilized to estimate crosstalk parameters ( $\beta, \theta$ ) and to perform device-level simulations as in [22]. However, in this article we are interested in error rates that can be ported to noisy circuit simulators and hence, stick to SRB and IDT protocols. Although, we experimentally collect SRB error rates for simultaneous 1-qubit gates and simultaneous 2- and 1-qubits gates as well, they show a smaller amount of change in error rates than two simultaneous 2-qubit gates. They are omitted for brevity.

IDT and SRB have different sets of advantages and limitations. On one hand, SRB can provide information about *parallel-context-dependence*, i.e., the impact of one gate (e.g., CNOT on Qa, Qb) on the error rate of another specific gate (e.g., CNOT on Qc, Qd). On the other hand, IDT provides the error rate of IDLE operation. However, IDT presents a more detailed nature of the error mechanism with both error-types and rates whereas SRB averages out every error as depolarizing (uniform Stochastic) error. Besides, IDT can provide information about both quantum and classical crosstalks.

### C. SIMULATION SETUP

#### 1) BENCHMARKS

Next, we simulate 9 quantum benchmarks (circuits) consisting of 3-qubit Fredkin gate (frdkn3), 3 and 4- qubit Grover search (grvr3 and grvr4), 4-qubit Hidden-Shift algorithm (hs4), 3 and 5-qubit quantum approximate optimization algorithm (qaoa3 and qaoa5), and three 5-qubit synthetic benchmarks (syn10, syn20, and syn30). The synthetic benchmarks are created with 2 CNOT gates (on (Q0,Q1) and (Q3,Q4)) and 1 Hadamard gate (on Q2) in each layer. The layer is repeated from 10, 20, and 30 times in syn10, syn20, and syn30 respectively. The synthetic benchmarks are created to maximize parallel gate operations and hence, crosstalk.

#### 2) SIMULATION CONDITIONS

The benchmarks are simulated for four different conditions: (1) with only crosstalk from IDT, (2) with only gate error,

(3) with gate errors from SRB (note: SRB error rates incorporate both gate error and crosstalk effect due to parallel gate operation), and (4) with gate error and crosstalk (from IDT).

#### 3) SIMULATORS

Cases (1) and (4) are simulated using the pyGSTi simulator [13], [14]. To simulate (IDT) crosstalk (case – 1), we use `build_cloud_crosstalk_model` method of pyGSTi. We specify the error rates as error dictionary in the crosstalk model. Interested readers can refer to this [23] pyGSTi tutorial to learn more about how to specify an error dictionary. A sample dictionary is added in the GitHub repository [18] for this article. The error dictionary is extracted from the `results` object from IDT experiments. The error dictionary specifies what are various error rates on spectator qubits due to CNOT operation on a pair of qubits. For example, the sample error dictionary file in the GitHub repository [18] contains error rates on Q2, Q3, and Q4 due to CNOT drive on Q0 and Q1. A value of `'SZZ:3,4': 0.0033` in the dictionary means a Stochastic ZZ type error of rate 0.0033 on Q3 and Q4 from CNOT on Q0 and Q1.

To simulate crosstalk and gate error together (case – 4), we add gate error as a depolarizing error to the aforementioned error dictionary for crosstalk. For example, to account for the gate error of CNOT (Q0, Q1), following Stochastic Pauli error types are added to the dictionary: `'SIX:0,1, 'SIY:0,1, 'SIZ:0,1, 'SXI:0,1, 'SYI:0,1, 'SZI:0,1, 'SXX:0,1, 'SXY:0,1, 'SXZ:0,1, 'SYX:0,1, 'SYY:0,1, 'SYZ:0,1, 'SZX:0,1, 'SZY:0,1, 'SZZ:0,1'`. The gate error rate is equally divided among these types to mimic depolarizing error.

Cases (2) and (3) are simulated using QASM Simulator from IBM Qiskit [24], [25]. The gate error is simulated with depolarizing error. However, QASM Simulator does not directly support conditional error rate simulation necessary for simulating crosstalk with SRB error rates. To overcome the limitation, we develop a *wrapper* that uses the QASM Simulator as the backend. The wrapper

- 1) takes a noiseless quantum circuit;
- 2) tracks parallel operations in each layer of the circuit;
- 3) selects appropriate error rate(s);
- 4) adds depolarizing error operator after each gate to create a noisy version of the circuit.

For example, if there is only one 2-qubit gate, e.g., CNOT(0, 1), in a layer, then the wrapper will pick 0.0214 as error rate and if there are two 2-qubit gates e.g., CNOT(0, 1) and CNOT(3, 4) in the layer, the wrapper will pick 0.0253 and 0.0296 respectively (Fig. 3).

#### 4) COMPARISON METRIC

We take Total Variation Distance (TVD) [Fig. 1(e)] to quantify the impact on errors on the outcome. TVD measures the deviation of a noisy outcome from the ideal (higher TVD indicates more impact).



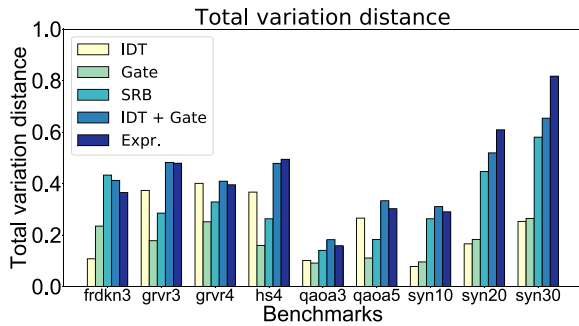


FIG. 4. Total variation distance for various benchmarks.

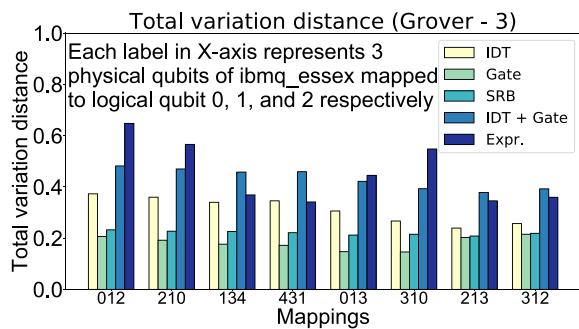


FIG. 5. Total variation distance for different mappings.

## 5) SIMULATION RESULTS AND DISCUSSION

Fig. 4 shows the simulated TVDs. We also plot experimental TVDs of benchmarks collected from `ibmq_essex`. Readout error is suppressed in experimental data using measurement calibration protocols [24] for a fair comparison with simulation. Besides, experimental results are averaged over 20 runs each with 8192 shots.

Our simulation clearly shows that considering only the gate error results in a high deviation from the experimental result. The average mismatch between gate error simulations and experiments is 26%. If we consider crosstalk (from SRB), the mismatch is reduced to 12.48% meaning crosstalk plays a significant role in NISQ computers. Furthermore, when we consider crosstalk errors (types and rates) from IDT and gate error, the simulation shows the best match with the experiment with an average mismatch of 4.52%.

Next, we extend our analysis to show the impact of different mappings [26]–[28] on crosstalk error. We choose 3-qubit `grvr3` benchmark and allocate 3 circuit (logical) qubits to physical qubits in 8 different ways known as maps. We present the results from both simulations (for 4 cases as before) and experiments. Here, gate error with IDT crosstalk shows the best match with experiments (8.9% mismatch) whereas the mismatch is 23.25% for SRB and 27% for gate error.

The study proves that existing analysis considering (and prioritizing) gate error is not sufficient. Crosstalk needs to be considered to devise better noise resilient techniques. Moreover, crosstalk characterization using techniques like IDT

gives more information about the error-types, and rates are more practical than SRB which averages out various types of errors as depolarizing error. In this article, we use IDT to approximate crosstalk on different gates as crosstalk on IDLE operation. Extending IDT to characterize crosstalk on active gates other than IDLE may match the experiments more closely. Thus, there are scopes to refine the crosstalk characterization protocol(s) to better match the experiments.

## V. CONCLUSION

In this article, we experimentally extract crosstalk error rates from NISQ computers using IDT and SRB, and present analysis with crosstalk. Our analysis shows that: (i) existing works on error resilience prioritizing only the gate error cannot capture NISQ behavior well and (ii) the IDT can model crosstalk more accurately compared to SRB.

## ACKNOWLEDGEMENT

The authors would like to thank Dr. Robin Blume-Kohout (Quantum Performance Lab, Sandia National Laboratories) for insightful discussions on Idle Tomography, Dr. Erik Nielsen, Dr. Kenneth Rudinger, and other developers (Quantum Performance Lab, Sandia National Laboratories) of the `pyGSTi` for the software package, and Dr. Christian Kraglund Andersen (ETH Zurich) for helpful discussions on crosstalk in NISQ devices.

## REFERENCES

- [1] J. Preskill, “Quantum computing in the nisyq era and beyond,” *Quantum*, vol. 2, p. 79, Aug. 2018, doi: [10.22331/q-2018-08-06-79](https://doi.org/10.22331/q-2018-08-06-79).
- [2] K. Rudinger, T. Proctor, D. Langharst, M. Sarovar, K. Young, and R. Blume-Kohout, “Probing context-dependent errors in quantum processors,” *Phys. Rev. X*, vol. 9, Jun. 2019, Art. no. 021045, doi: [10.1103/PhysRevX.9.021045](https://doi.org/10.1103/PhysRevX.9.021045).
- [3] R. Blume-Kohout, E. Nielsen, K. Rudinger, K. Young, M. Sarovar, and T. Proctor, “Idle tomography: Efficient gate characterization for N-qubit processors,” in *Proc. APS Mar. Meeting Abstracts*, ser. APS Meeting Abstracts, vol. 2019, Jan. 2019, Paper P35.006. [Online]. Available: <https://www.osti.gov/biblio/1581878-idle-tomography>
- [4] J. M. Gambetta et al., “Characterization of addressability by simultaneous randomized benchmarking,” *Phys. Rev. Lett.*, vol. 109, Dec. 2012, Art. no. 240504, doi: [10.1103/PhysRevLett.109.240504](https://doi.org/10.1103/PhysRevLett.109.240504).
- [5] A. Erhard et al., “Characterizing large-scale quantum computers via cycle benchmarking,” *Nature Commun.*, vol. 10, no. 1, Nov. 2019, doi: [10.1038/s41467-019-13068-7](https://doi.org/10.1038/s41467-019-13068-7).
- [6] T. J. Proctor, A. Carignan-Dugas, K. Rudinger, E. Nielsen, R. Blume-Kohout, and K. Young, “Direct randomized benchmarking for multi-qubit devices,” *Phys. Rev. Lett.*, vol. 123, Jul. 2019, Art. no. 030503, doi: [10.1103/PhysRevLett.123.030503](https://doi.org/10.1103/PhysRevLett.123.030503).
- [7] R. Harper, S. T. Flammia, and J. J. Wallman, “Efficient learning of quantum noise,” *Nature Phys.*, Aug. 2020, doi: [10.1038/s41567-020-0992-8](https://doi.org/10.1038/s41567-020-0992-8).
- [8] J. Heinsoo et al., “Rapid high-fidelity multiplexed readout of superconducting qubits,” *Phys. Rev. Appl.*, vol. 10, Sep. 2018, Art. no. 034040, doi: [10.1103/PhysRevApplied.10.034040](https://doi.org/10.1103/PhysRevApplied.10.034040).
- [9] D. M. Abrams, N. Didier, S. A. Caldwell, B. R. Johnson, and C. A. Ryan, “Methods for measuring magnetic flux crosstalk between tunable transmons,” *Phys. Rev. Appl.*, vol. 12, Dec. 2019, Art. no. 064022, doi: [10.1103/PhysRevApplied.12.064022](https://doi.org/10.1103/PhysRevApplied.12.064022).
- [10] A. Winick, J. J. Wallman, and J. Emerson, “Simulating and mitigating crosstalk,” 2020, *arXiv:quant-ph/2006.09596*.
- [11] S. Krinner et al., “Benchmarking coherent errors in controlled-phase gates due to spectator qubits,” 2020, *arXiv:quant-ph/2005.05914*.

- [12] P. Murali, D. C. McKay, M. Martonosi, and A. Javadi-Abhari, "Software mitigation of crosstalk on noisy intermediate-scale quantum computers," in *Proc. 25th Int. Conf. Architectural Support Program. Lang. Operating Syst.*, Mar. 2020, doi: [10.1145/3373376.3378477](https://doi.org/10.1145/3373376.3378477).
- [13] E. Nielsen *et al.*, "pygstio/pygsti: Version 0.9.9.1," Feb. 2020, doi: [10.5281/zenodo.3675466](https://doi.org/10.5281/zenodo.3675466).
- [14] E. Nielsen, K. Rudinger, T. Proctor, A. Russo, K. Young, and R. Blume-Kohout, "Probing quantum processor performance with pyGSTi," *Quantum Sci. Technol.*, vol. 5, no. 4, Jul. 2020, Art. no. 044002, doi: [10.1088/2058-9565/ab8aa4](https://doi.org/10.1088/2058-9565/ab8aa4).
- [15] E. Magesan and J. M. Gambetta, "Effective hamiltonian models of the cross-resonance gate," *Phys. Rev. A*, vol. 101, May 2020, Art. no. 052308, doi: [10.1103/PhysRevA.101.052308](https://doi.org/10.1103/PhysRevA.101.052308).
- [16] J. Ku *et al.*, "Suppression of unwanted zz interactions in a hybrid two-qubit system," 2020, *arXiv:quant-ph/2003.02775*.
- [17] M. Sarovar, T. Proctor, K. Rudinger, K. Young, E. Nielsen, and R. Blume-Kohout, "Detecting crosstalk errors in quantum information processors," 2019, *arXiv:quant-ph/1908.09855*.
- [18] A. A. Saki. SRB and IDT experiments for crosstalk extraction. Accessed: Aug. 15, 2020. [Online]. Available: <https://github.com/ashsaki/Crosstalk-experiments>
- [19] E. Knill *et al.*, "Randomized benchmarking of quantum gates," *Phys. Rev. A*, vol. 77, Jan. 2008, Art. no. 012307, doi: [10.1103/PhysRevA.77.012307](https://doi.org/10.1103/PhysRevA.77.012307).
- [20] S. Sheldon, E. Magesan, J. M. Chow, and J. M. Gambetta, "Procedure for systematically tuning up cross-talk in the cross-resonance gate," *Phys. Rev. A*, vol. 93, Jun. 2016, Art. no. 060302, doi: [10.1103/PhysRevA.93.060302](https://doi.org/10.1103/PhysRevA.93.060302).
- [21] IBM. IBM Quantum Experience. Accessed: Aug. 15, 2020. [Online]. Available: <https://quantum-computing.ibm.com/>
- [22] N. Lacroix *et al.*, "Improving the performance of deep quantum optimization algorithms with continuous gate sets," 2020, *arXiv:quant-ph/2005.05275*.
- [23] pyGSTi. Implicit Models. Accessed: Aug. 15, 2020. [Online]. Available: [https://github.com/pyGSTi/pyGSTi/blob/master/jupyter\\_notebooks/Tutorials/objects/ImplicitModel.ipynb](https://github.com/pyGSTi/pyGSTi/blob/master/jupyter_notebooks/Tutorials/objects/ImplicitModel.ipynb)
- [24] J. Gambetta *et al.*, "Qiskit/qiskit: Qiskit 0.19.3," Jun. 2020, doi: [10.5281/zenodo.3873240](https://doi.org/10.5281/zenodo.3873240).
- [25] IBM. Simulating a quantum circuit with noise. Accessed: Aug. 15, 2020. [Online]. Available: [https://qiskit.org/documentation/tutorials/simulators/2\\_device\\_noise\\_simulation.html#Simulating-a-quantum-circuit-with-noise](https://qiskit.org/documentation/tutorials/simulators/2_device_noise_simulation.html#Simulating-a-quantum-circuit-with-noise)
- [26] S. S. Tannu and M. K. Qureshi, "Not all qubits are created equal: A case for variability-aware policies for nisq-era quantum computers," in *Proc. 24th Int. Conf. Architectural Support Program. Languages Operating Syst. (ASPLOS '19)*, 2019, pp. 987–999, doi: [10.1145/3297858.3304007](https://doi.org/10.1145/3297858.3304007).
- [27] A. A. Saki, M. Alam, and S. Ghosh, "QURE: Qubit re-allocation in noisy intermediate-scale quantum computers," in *Proc. 56th Annu. Des. Automat. Conf. (DAC '19)*, 2019, pp. 1–6, doi: [10.1145/3316781.3317888](https://doi.org/10.1145/3316781.3317888).
- [28] P. Murali, J. M. Baker, A. Javadi-Abhari, F. T. Chong, and M. Martonosi, "Noise-adaptive compiler mappings for noisy intermediate-scale quantum computers," in *Proc. 24th Int. Conf. Architectural Support Program. Languages Operating Syst. (ASPLOS '19)*, Apr. 2019, pp. 1015–1029, doi: [10.1145/3297858.3304075](https://doi.org/10.1145/3297858.3304075).